Deficiency of Stat1 in CD11c$^+$ Cells Alters Adipose Tissue Inflammation and Improves Metabolic Dysfunctions in Mice Fed a High-Fat Diet

Antu Antony,[1] Zeqin Lian,[1] Xiaoyuan Dai Perrard,[1] Jerry Perrard,[1] Hua Liu,[1] Aaron R. Cox,[1] Pradip Saha,[1,2] Lothar Hennighausen,[3] Sean M. Hartig,[1,2] Christie M. Ballantyne,[1,4,5] and Huaizhu Wu[1,4]

Diabetes 2021;70:720–732 | https://doi.org/10.2337/db20-0634

CD11c$^+$ macrophages/dendritic cells (MDCs) are increased and display the classically activated M1-like phenotype in obese adipose tissue (AT) and may contribute to AT inflammation and insulin resistance. Stat1 is a key transcription factor for MDC polarization into the M1-like phenotype. Here, we examined the role of Stat1 in obesity-induced AT MDC polarization and inflammation and insulin resistance using mice with specific knockout of Stat1 in MDCs (cKO). Stat1 was upregulated and phosphorylated, indicating activation, early and persistently in AT and AT MDCs of wild-type mice fed a high-fat diet (HFD). Compared with littermate controls, cKO mice fed an HFD (16 weeks) had reductions in MDC (mainly CD11c$^+$ macrophage) M1-like polarization and interferon-γ–expressing T-helper type 1 (Th1) cells but increases in interleukin 5–expressing Th2 cells and eosinophils in perigonadal and inguinal AT, and enhanced inguinal AT browning, with increased energy expenditure. cKO mice compared with controls also had significant reductions in triglyceride content in the liver and skeletal muscle and exhibited improved insulin sensitivity and glucose tolerance. Taken together, our results demonstrate that Stat1 in MDCs plays an important role in obesity-induced MDC M1-like polarization and AT inflammation and contributes to insulin resistance and metabolic dysfunctions in obese mice.

Obesity is a major risk factor for type 2 diabetes, fatty liver disease, and many other diseases (1). Obesity causes adipose tissue (AT) expansion and inflammation, which contributes to insulin resistance and type 2 diabetes (2–4). Increased number of macrophages is a hallmark of AT inflammation in obesity (5–7). Furthermore, macrophages in obese AT express high levels of CD11c (8–10), a β2-integrin that is usually expressed on mouse dendritic cells (DCs) and a subpopulation of monocytes and macrophages (11). CD11c$^+$ cells in AT include CD11c$^+$ macrophages and DCs (which are all CD11c$^+$) (12) and are here referred to as macrophages/DCs (MDCs). MDCs in obese AT exhibit classically activated M1-like proinflammatory phenotypes and are the major contributors to obesity-induced AT inflammation (8–10,12–15). However, the transcriptional mechanism for MDC M1-like polarization in obese AT remains poorly understood.

Signal transducer and activator of transcription 1 (Stat1) is a key transcription factor for macrophage polarization into the M1-like phenotype (16). To be functional, Stat1 needs to be phosphorylated mainly by Janus kinase 1 (Jak1) and Jak2 (17). Stat1 then dimerizes, translocates into the nucleus, and regulates expression of a large number of proinflammatory molecules (17,18). Interferon-γ (IFN-γ), which is mainly produced by CD4$^+$ T-helper type 1 (Th1) and effector CD8$^+$ T cells and is increased in AT in obesity (19–21), is the primary inducer to activate Jak/Stat1 signaling (17). Toll-like receptor 2 (TLR2)– and TLR4-mediated pathways, which are induced in obese AT (22,23), also activate Stat1 signaling (18). Nevertheless, a potential role of Stat1 in obesity-linked AT MDC polarization and inflammation and metabolic functions has not been reported.

[1]Department of Medicine, Baylor College of Medicine, Houston, TX
[2]Department of Molecular and Cellular Biology, Baylor College of Medicine, Houston, TX
[3]Laboratory of Genetics and Physiology, National Institute of Diabetes and Digestive and Kidney Diseases, Bethesda, MD
[4]Department of Pediatrics, Baylor College of Medicine, Houston, TX
[5]Center for Cardiometabolic Disease Prevention, Baylor College of Medicine, Houston, TX

Corresponding author: Huaizhu Wu, hwu@bcm.edu

Received 20 June 2020 and accepted 2 December 2020

This article contains supplementary material online at https://doi.org/10.2337/figshare.13348094.

A.A. and Z.L. contributed equally to this work.

In the current study, we aimed to examine the role of Stat1 in obesity-induced AT $CD11c^+$ MDC polarization and inflammation and in metabolic functions in mice.

RESEARCH DESIGN AND METHODS

Animal Care and Use

Wild-type (WT) C57BL/6J mice purchased from The Jackson Laboratory (Bar Harbor, ME) were maintained in the animal facility at Baylor College of Medicine. Mice with Stat1 knockout in $CD11c^+$ cells (cKO) were generated by crossbreeding CD11c-Cre mice (Stock No. 008068; The Jackson Laboratory) and $Stat1^{fl/fl}$ mice (24). CD11c-$Cre^{+/-}$ $Stat1^{fl/fl}$ cKO mice and CD11c-$Cre^{-/-}Stat1^{fl/fl}$ littermate controls were co-housed in the same cages where possible and fed normal chow diet (ND) (12% kcal from fat) (PicoLab Rodent Diet 5010; Purina Mills, St. Louis, MO) after weaning until 8 weeks old. Then, mice were fed western high-fat diet (HFD) (41% kcal from fat) (Dyet 112734; Dyets Inc., Bethlehem, PA) for up to 16 weeks or maintained on ND for the same period. All mice were housed at room temperature (20–22°C) in a pathogen-free facility that maintained a 12-h light/12-h dark cycle throughout. For AT uncoupling protein 1 (UCP1) protein assay, mice were injected intraperitoneally with CL316,243 (Sigma-Aldrich, St. Louis, MO) at 1 mg/kg daily for 7 days. Total fat mass and lean mass were determined with a Lunar PIXImus small animal densitometer (GE Healthcare, Madison, WI). Perigonadal AT (pAT), inguinal AT (iAT), liver, and skeletal muscle were dissected and used for the study. Animal studies and procedures were approved by the institutional animal care and use committee of Baylor College of Medicine.

AT From Human Subjects

Omental AT was collected from 21 subjects with morbid obesity (20 females, 1 male; mean age 38.3 ± 1.8 years; mean BMI 49.9 ± 1.7 kg/m^2) at the time of bariatric surgery. Human studies were approved by the institutional review board of Baylor College of Medicine, and informed consent was obtained.

Metabolic Studies

Intraperitoneal glucose tolerance test (GTT) and insulin tolerance test (ITT) were performed, and insulin-stimulated Akt phosphorylation was examined in pAT, skeletal muscle, and liver tissues in mice after fasting for 6 h (19,20,25). Oxygen consumption and energy expenditure were examined in mice using Oxymax system cages (Columbus Instruments, Columbus, OH) for a total of 4 days after acclimation for 3 days. Triglyceride (TG) content in the liver and skeletal muscle was measured as described previously (19,20,25).

Flow Cytometry

Stromal vascular cells (SVCs) were isolated from pAT and iAT following digestion with collagenase type I (Worthington Biochemical Corporation, Lakewood, NJ) and under Fc receptor blockade with anti-mouse CD16/CD32 (BD Biosciences, San Jose, CA), stained with antibodies specific for various immune cell markers (Supplementary Table) or respective isotype controls. For intracellular detection of cytokines, SVCs were incubated with Leukocyte Activation Cocktail (BD Biosciences) or lipopolysaccharide (200 ng/mL) and Golgi Plug (BD Biosciences) in complete RPMI medium for 4–12 h and then fixed and permeabilized with Cytofix/Cytoperm kit (BD Biosciences) and stained for various cytokines (19–21,25). For Foxp3 staining, SVCs were fixed and permeabilized using a Foxp3/Transcription Factor Staining Buffer Kit (Thermo Fisher Scientific, Waltham, MA). Data were collected with an LSR II Flow Cytometer (BD Biosciences) and analyzed using Kaluza software (Beckman Coulter, Indianapolis, IN). Viable $CD45^+$ cells were first gated. Within viable $CD45^+$ cells, total macrophages and DCs were identified as $F4/80^{+/high}$ cells, which were classified into $CD11c^+/CD206^{-/low}$ M1-like MDCs and $CD206^+/CD11c^-$ M2-like macrophages and examined for intracellular expression of interleukin 12 (IL-12) and tumor necrosis factor-α (TNF-α). In a separate experiment, on the basis of CD64 expression (12), $CD11c^+$ MDCs were separated into $CD11c^+CD64^+$ macrophages and $CD11c^+CD64^-$ DCs, which were further examined for expression of IL-12 and TNF-α. Total T cells were identified as $CD3^+$ cells, within which $CD4^+$ and $CD8^+$ T cells were quantified and examined for intracellular expression of IFN-γ and IL-5. Regulatory T cells (Tregs) were defined as $Foxp3^+CD25^+$ cells within $CD4^+$ T cells. Eosinophils were identified as $CD170^+$ cells. Data were presented as cell numbers per gram AT calculated by using counting beads (BioLegend, San Diego, CA) or as percentages of cell subsets in certain cell types. Macrophages, DCs, and T cells were also examined in splenocytes (26).

Cell Isolation

After collagenase digestion of pAT, adipocytes were floated and isolated, and SVCs were pelleted by centrifugation. MDCs were isolated from SVCs using FITC-conjugated anti-mouse CD11c antibody (BioLegend) and FITC Positive Selection Kit II (STEMCELL Technologies, Cambridge, MA); the rest of the SVCs were also used.

Immunohistochemistry

Paraformaldehyde-fixed paraffin-embedded tissue sections were stained with hematoxylin and eosin or processed for immunostaining for UCP1 (19–21,25). Images of stained tissue sections were captured using a microscope coupled with NIS-Elements software (Nikon Eclipse Ci; Nikon Instruments, Melville, NY) and analyzed using ImageJ software.

RNA Isolation and Quantitative RT-PCR

Total RNA was isolated from tissues using TRIzol Reagent (Thermo Fisher Scientific). Gene expression was examined by quantitative RT-PCR (RT-qPCR) using predesigned

primers and probes (Thermo Fisher Scientific) and expressed as relative mRNA levels to 18S rRNA internal control.

Western Blotting

Tissues or isolated cell fractions were homogenized in cOmplete Lysis-M EDTA-free buffer (MilliporeSigma, St. Louis, MO). Western blotting was performed for Ser^{473}-phosporylated (pAkt), Tyr^{701}-phosphorylated Stat1 (pStat1), total Akt (tAkt), total Stat1 (tStat1), tubulin, and β-actin (19,20,25).

In Vivo Neutralization of IL-5

cKO mice on HFD for 12 weeks (or WT on ND) started to receive intraperitoneal injections of 40 μg of anti-mouse/human IL-5 antibody or isotype control (BioLegend) once every 72 h for a total of up to 11 injections. ITT and GTT were performed at 2 days after 9 and 10 injections, respectively. Mice were euthanized at 2 days after 11 injections (or 2 injections in WT mice). pAT and iAT were harvested for further analyses.

Statistics

All data are presented as mean ± SD and were tested for normal distribution and equivalence of variance. Unpaired Student *t* test or Mann-Whitney *U* test (for comparisons between two groups) or one-way ANOVA or Kruskal-Wallis test followed by post hoc pairwise comparisons (for three or more groups) was used for statistical analysis performed in GraphPad Prism 8.3. Pearson correlation coefficient was computed to examine correlations. $P \leq 0.05$ was considered statistically significant.

Data and Resource Availability

All data generated or analyzed during this study are included in the published article (and its Supplementary Material). The mouse model generated and/or analyzed during the current study is available from the corresponding author upon reasonable request.

RESULTS

Stat1 in AT and AT MDCs of WT Mice Fed HFD and in AT of Obese Humans

We first observed that after HFD feeding in WT mice, Stat1 was upregulated and phosphorylated early (within 1 week of HFD) and persistently (at 16 weeks on HFD) in pAT (Fig. 1*A*). Further analysis indicated that Stat1 was elevated early and persistently in pAT MDCs (CD11c$^+$) (Fig. 1*B*) and adipocytes of WT mice fed HFD (Fig. 1*C*). Furthermore, STAT1 mRNA levels were positively correlated with CD11c levels in visceral AT of humans with morbid obesity (Fig. 1*D*).

Generation and Characterization of cKO Mice

Next, we generated mice with Stat1 knockout in CD11c$^+$ cells (cKO) to examine the role of MDC Stat1 in obesity. Compared with littermate controls, cKO mice had reduced mRNA levels of Stat1 in pAT and iAT and specific ablation of Stat1 in CD11c$^+$ MDCs (Fig. 2*A* and *B*). When fed ND, cKO mice compared with controls showed no differences in body weight, total fat and lean mass, and weight and ratios to body weight of pAT pads and liver (Fig. 2*C*–*G*). HFD feeding resulted in comparable weight gain in cKO and control mice (Fig. 2*C*). At 16 weeks on HFD, cKO mice and controls had similar total fat and lean mass and pAT size, but cKO mice had smaller livers (Fig. 2*D*–*G*). Therefore, Stat1 ablation in MDCs in mice leads to no changes in HFD-induced weight gain and fat mass but to smaller livers.

cKO Mice on HFD Exhibit an Improved Phenotype of Macrophages and DCs in pAT and iAT

Flow cytometric analysis showed that total F4/80$^+$ macrophages and DCs in both pAT and iAT were not significantly different between cKO mice and controls fed HFD for 16 weeks (Fig. 3*A* and *B*). Within the total F4/80$^+$ cells of pAT, the percentage of CD11c$^+$ M1-like MDCs was reduced and the percentage of CD206$^+$ M2-like macrophages increased, leading to a significantly reduced ratio of M1- to M2-like macrophages and DCs in obese cKO mice compared with obese controls (Fig. 3*A*). In contrast, these changes did not occur in iAT (Fig. 3*B*). In obese control mice, CD11c$^+$ MDCs in pAT and iAT compared with CD11c$^-$ macrophages expressed higher levels of type 1 cytokines, including IL-12 (Fig. 3*C* and *D*) and TNF-α (data not shown), consistent with a proinflammatory phenotype. Importantly, compared with those in obese controls, CD11c$^+$ MDCs in pAT and iAT of obese cKO mice expressed lower levels of IL-12 and TNF-α (Fig. 3*C* and *D*).

Further analysis revealed that CD11c$^+$CD64$^+$ macrophages accounted for the majority of CD11c$^+$ MDCs in pAT and iAT of both controls and cKO mice (Fig. 3*E* and *F*), consistent with another report (12). cKO and control mice did not show significant differences in the proportions of macrophages and DCs within CD11c$^+$ MDCs in pAT and iAT (Fig. 3*E* and *F*). In obese controls, CD11c$^+$ macrophages compared with DCs in pAT and iAT expressed higher levels of IL-12 and TNF-α (Fig. 3*G* and *H*). CD11c$^+$ macrophages, but not DCs, in pAT and iAT of obese cKO versus control mice showed significant reductions in IL-12 and TNF-α levels (Fig. 3*G* and *H*). Compared with obese controls, cKO mice tended to have lower MHC-II on DCs but not on macrophages in pAT and iAT (Supplementary Fig. 1). However, the difference in DC MHC-II levels did not reach statistical significance.

Gene expression analysis showed that M1-like macrophage markers, such as IL-12, TNF-α, MCP-1, and interferon regulatory factor 5, were reduced, and M2-like markers, including CD206 and interferon regulatory factor 4, tended to be increased in AT, particularly pAT, of cKO mice compared with controls (Fig. 3*I* and *J*). These data suggest that Stat1 ablation in MDCs mainly improves macrophage phenotype, with reductions in M1-like macrophages and a trend toward increases in M2-like macrophages, in AT of mice with obesity.

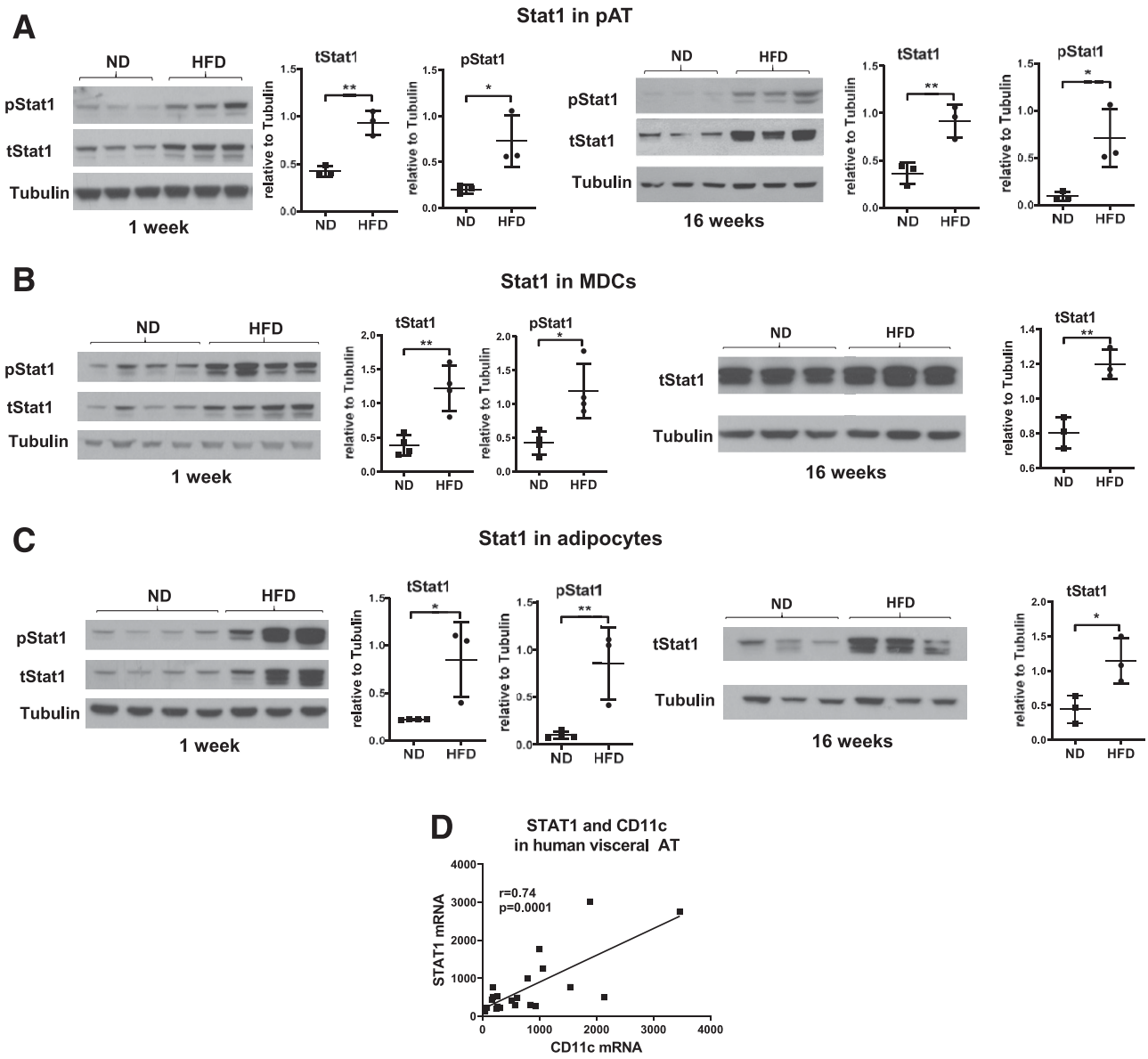

Figure 1—HFD in WT mice increases Stat1 levels and phosphorylation in pAT and CD11c$^+$ MDCs and adipocytes from pAT. tStat1 and pStat1 levels examined by Western blotting in pAT (*A*) and MDCs (*B*) and adipocytes (*C*) from pAT of male WT C57BL/6J mice fed ND or HFD for 1 week or 16 weeks. Correlation of mRNA levels of STAT1 and CD11c in visceral AT from obese humans (*D*). Data are mean ± SD. *$P <$ 0.05, **$P < 0.01$.

T-Cell–Related Inflammation Is Altered in pAT and iAT of cKO Mice on HFD

Given the role of T cells in AT inflammation and metabolic function (10,15,21,27–31), we examined AT T cells and related inflammation. Flow cytometric analysis showed no changes in total T-cell numbers in pAT or iAT of HFD-fed cKO mice compared with controls (Fig. 4*A* and *B*). Within total T cells in pAT, the proportion of CD8$^+$ T cells, which showed greater increases than CD4$^+$ T cells in pAT of obese versus lean WT mice (19,27), was significantly reduced, whereas no change was noted in the proportion of CD4$^+$ cells in obese cKO mice compared with controls (Fig. 4*A*). Within CD4$^+$ T cells, the percentage of IFN-γ–expressing Th1 cells diminished, the percentage of IL-5–expressing Th2 cells increased, and Tregs did not change significantly in pAT and iAT of obese cKO mice compared with controls (Fig. 4*C* and *D*). Gene expression analysis showed that CD8 and IFN-γ were reduced and IL-5 tended to be increased in pAT and iAT of obese cKO mice compared with controls (Fig. 4*E* and *F*). Therefore, Stat1 ablation in MDCs alters T-cell inflammation, with reduced Th1 and CD8$^+$ T cells, but increased Th2 cells, in AT with obesity. In contrast, obese cKO mice compared with controls did not show significant changes in macrophages, DCs, and T cells in spleens (Supplementary Fig. 2).

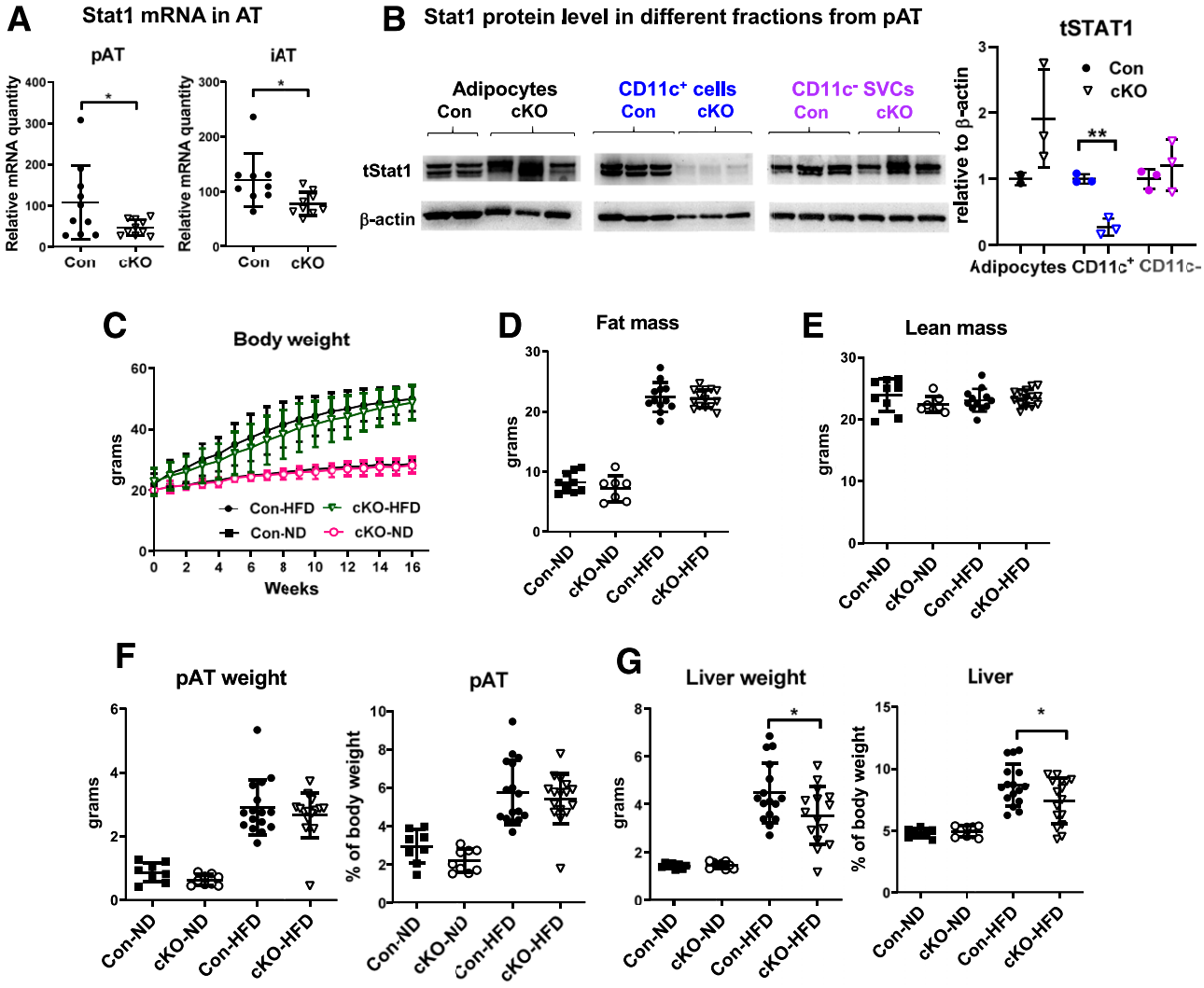

Figure 2—cKO mice do not have altered HFD-induced weight gain and fat mass but have reduced liver weight. Stat1 mRNA in pAT and iAT (*A*) and Stat1 protein levels in adipocytes, CD11c$^+$ MDCs, and CD11c$^-$ SVCs isolated from pAT (*B*) of male cKO mice and littermate controls fed HFD (16 weeks). Body weight changes of male cKO mice and littermate controls fed HFD or ND (*C*). Total fat mass (*D*) and lean mass (*E*) determined with a PIXImus small animal densitometer and weight and relative ratio to body weight of the pAT pad (*F*) and liver (*G*) of male cKO mice and littermate controls fed ND or HFD (16 weeks). *$P < 0.05$. Con, control.

Eosinophils Are Expanded in pAT and iAT of cKO Mice on HFD

Eosinophils are enriched in AT of lean WT mice and decrease with obesity (32). Gene expression analysis showed that obese cKO mice compared with controls had upregulation of the eosinophil marker CD170 in pAT and iAT (Fig. 4*G* and *H*). Flow cytometric analysis confirmed the increases in eosinophils in pAT and iAT of obese cKO mice versus controls (Fig. 4*G* and *H*). Furthermore, this change was specific to AT, with no significant differences in blood or bone marrow eosinophils between cKO mice and controls (Supplementary Fig. 3*A* and *B*).

cKO Mice Fed HFD Have Promoted Browning/Beige Adipogenesis and Improved Energy Metabolism

cKO mice compared with controls on HFD had smaller adipocytes in pAT and iAT (Fig. 5*A*). Notably, browning/beige adipogenesis markers, such as UCP1, CIDEA, and Prdm16, were upregulated in iAT of obese cKO mice compared with controls (Fig. 5*B*), but the levels in pAT were undetectably low in both cKO and control mice (data not shown). Upon treatment with the β3-agonist (CL316,243), cKO mice on HFD showed significantly higher UCP1 levels in both pAT and iAT than control mice (Fig. 5*C*). Compared with controls, cKO mice fed HFD showed a significant increase in VO_2 (Fig. 5*D*), indicating higher energy expenditure; lower respiratory exchange ratio (Fig. 5*E*), indicating higher utilization of fat as energy source; and greater food intake (Fig. 5*F*) but no changes in activity (Fig. 5*G*). HFD-fed cKO mice compared with control mice had significant reductions in TG content in the liver and skeletal muscle (Fig. 5*H*). These data suggest that the changes in AT inflammation caused by Stat1 ablation in MDCs may improve AT

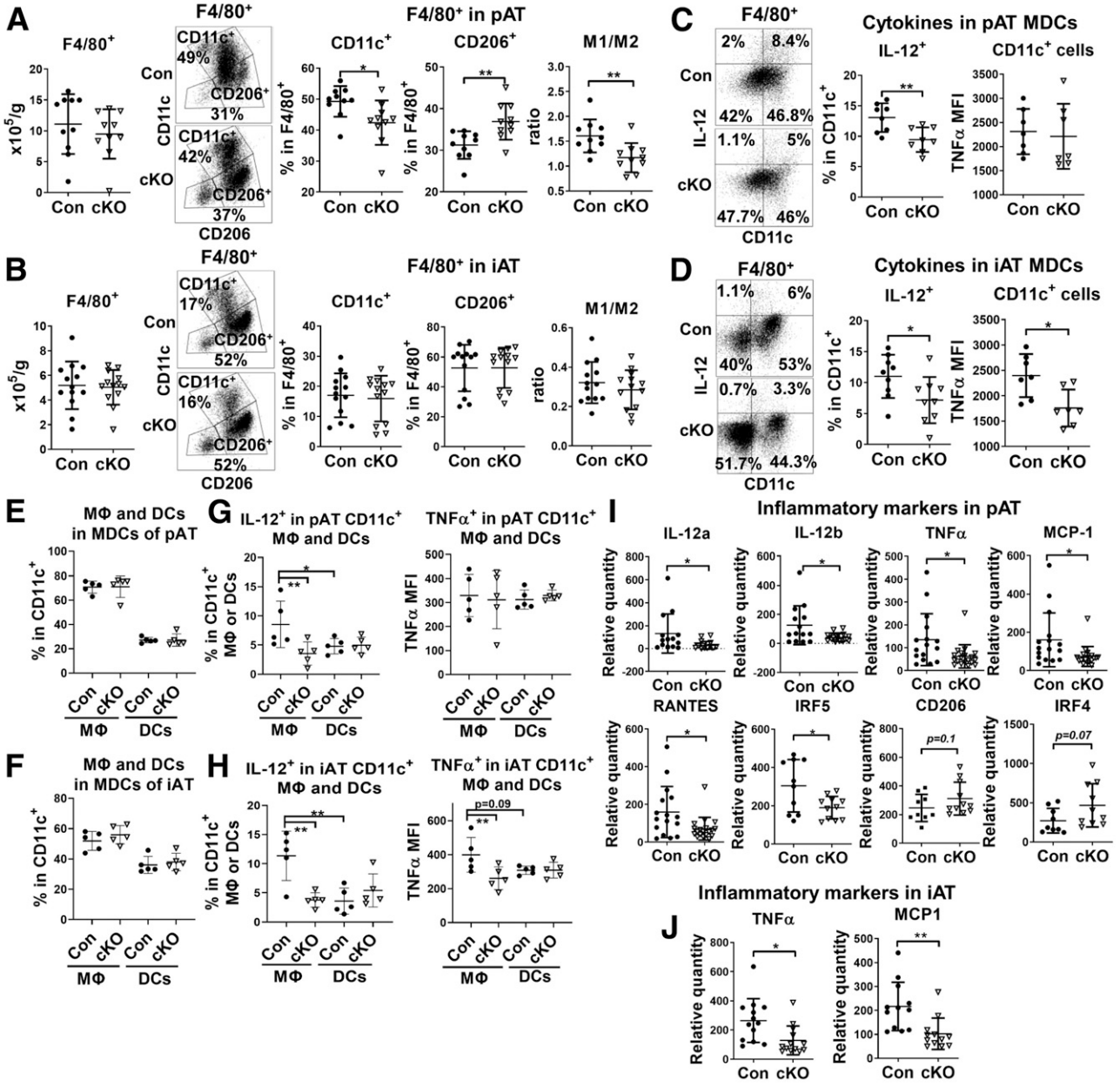

Figure 3—cKO mice on HFD exhibit an improved macrophage phenotype in pAT and iAT. Male cKO mice and littermate controls were fed HFD for 16 weeks. Flow cytometric analysis of F4/80$^+$ macrophages and DCs in SVCs isolated from pAT (*A* and *C*) and iAT (*B* and *D*) of cKO and control mice showing total F4/80$^+$ cells, percentages of CD11c$^+$ (M1-like MDC) and CD206$^+$ (M2-like macrophage) cells in F4/80$^+$ cells, ratio of CD11c$^+$ to CD206$^+$ cells (*A* and *B*), and intracellular levels of IL-12 and TNF-α in CD11c$^+$ (F4/80$^+$) MDCs (*C* and *D*). Flow cytometric analysis of CD11c$^+$CD64$^+$ macrophages and CD11c$^+$CD64$^-$ DCs with CD11c$^+$ MDCs of SVCs from pAT (*E* and *G*) and iAT (*F* and *H*) of cKO and control mice showing proportions of macrophages and DCs within MDCs (*E* and *F*) and intracellular levels of IL-12 and TNF-α in CD11c$^+$ macrophages and DCs (*G* and *H*). RT-qPCR gene expression analysis of pAT (*I*) and iAT (*J*) of cKO and control mice showing mRNA levels of M1- and M2-like markers and cytokines. *$P < 0.05$, **$P < 0.01$. Con, control; MFI, mean fluorescence intensity.

metabolism, with increased browning/beige adipogenesis, leading to enhanced energy expenditure and ameliorated ectopic lipid deposition in the liver and skeletal muscle.

cKO Mice on HFD Have Improved Insulin Sensitivity

Compared with controls, cKO mice on HFD had lower fasting plasma levels of glucose (Fig. 6*A*) and exhibited improved systemic insulin sensitivity and glucose tolerance as examined by ITT and GTT (Fig. 6*B* and *C*). Furthermore, insulin-stimulated Akt phosphorylation was significantly increased, indicating improved insulin sensitivity, in pAT, skeletal muscle, and liver from HFD-fed cKO mice compared with controls (Fig. 6*D*–*F*). These data suggest that Stat1 ablation in MDCs improves obesity-induced systemic and tissue-specific insulin resistance.

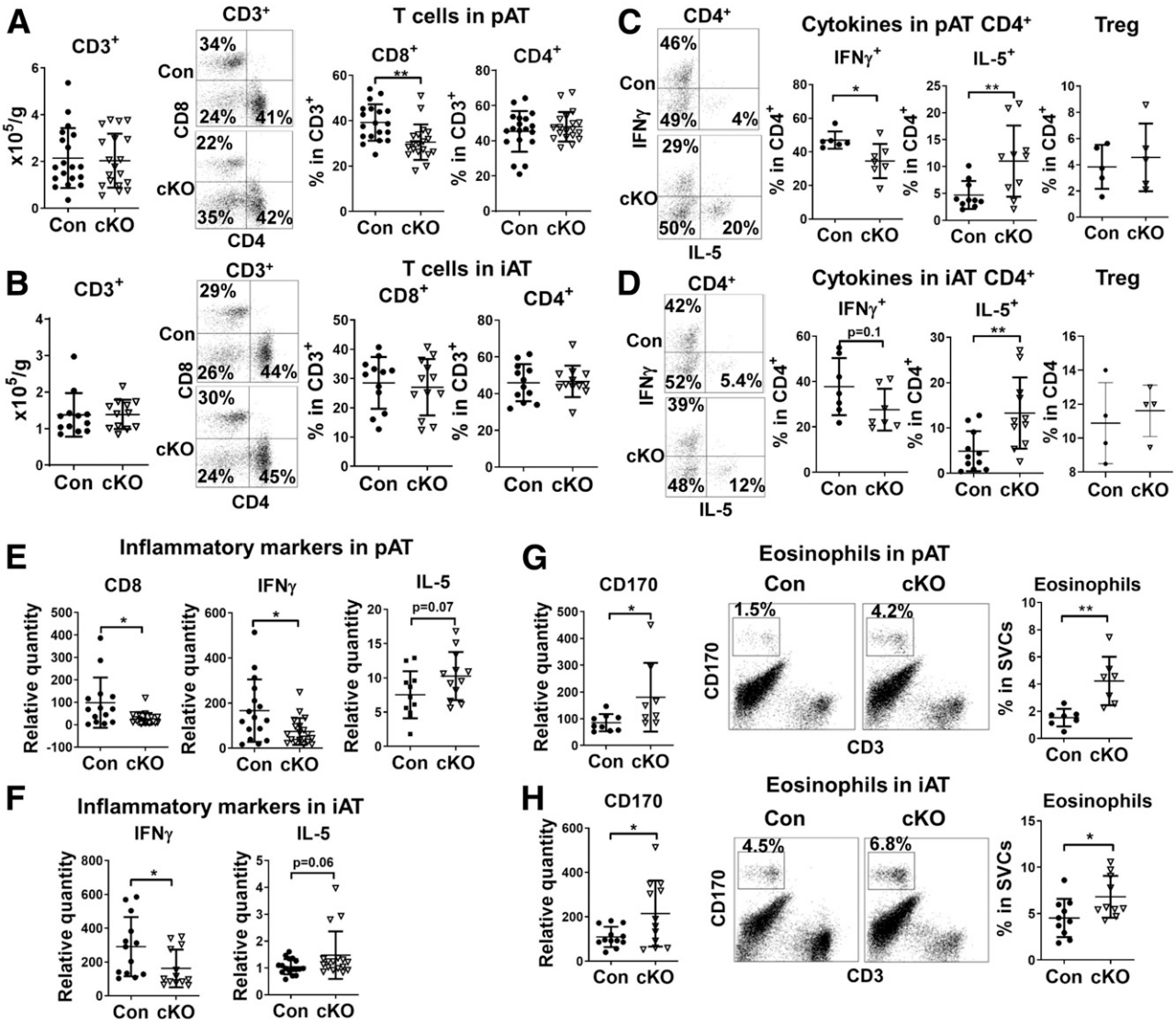

Figure 4—T-cell–mediated inflammation and eosinophils are altered in pAT and iAT of cKO mice fed HFD. Male cKO mice and littermate controls were fed HFD for 16 weeks. Flow cytometric analysis of T cells in SVCs isolated from pAT (*A* and *C*) and iAT (*B* and *D*) of cKO and control mice showing CD3$^+$ total T cell numbers, percentages of CD8$^+$ and CD4$^+$ T cells in total T cells (*A* and *B*), and intracellular expression of IFN-γ (for Th1), IL-5 (for Th2), and Tregs in CD4$^+$ T cells (*C* and *D*). RT-qPCR gene expression analysis of pAT (*E*) and iAT (*F*) of cKO and control mice showing mRNA levels of T-cell markers and cytokines. RT-qPCR and flow cytometry analyses of pAT (*G*) and iAT (*H*) of cKO and control mice showing eosinophils (CD170$^+$) and the related marker (CD170). *$P < 0.05$, **$P < 0.01$. Con, control.

Reducing Eosinophils in Obese cKO Mice Does Not Affect Insulin Sensitivity

Because of the reported protective role of eosinophils in obesity (32), we determined whether reducing AT eosinophils reverses the metabolic phenotype of cKO mice on HFD. A pilot study showed that two injections of an anti-IL-5 antibody in WT mice dramatically reduced eosinophils in pAT (Supplementary Fig. 4) and iAT (data not shown). Repetitively injecting the anti-IL-5 antibody for a total of 11 times in cKO mice that had been fed HFD for 12 weeks consistently induced drastic reductions in eosinophils in pAT and iAT (Fig. 7*A*). However, this change was not associated with significant alterations in systemic insulin sensitivity and glucose tolerance (Fig. 7*B* and *C*), AT content of macrophages and DCs and T cells, or AT expression of beiging markers in cKO mice (Fig. 7*D*–*F*).

DISCUSSION

Stat1 is a key transcription factor that regulates macrophage polarization into classically activated M1-like phenotypes (16). Here, we report our novel observations that Stat1 is upregulated and phosphorylated, indicating activation, early and persistently in AT and AT CD11c$^+$ MDCs in mice fed HFD and correlates positively with CD11c levels in visceral AT of obese humans and that Stat1 KO in CD11c$^+$ MDCs protects mice from obesity-induced AT inflammation, insulin resistance, and metabolic dysfunction. Thus, our current study demonstrates for the first

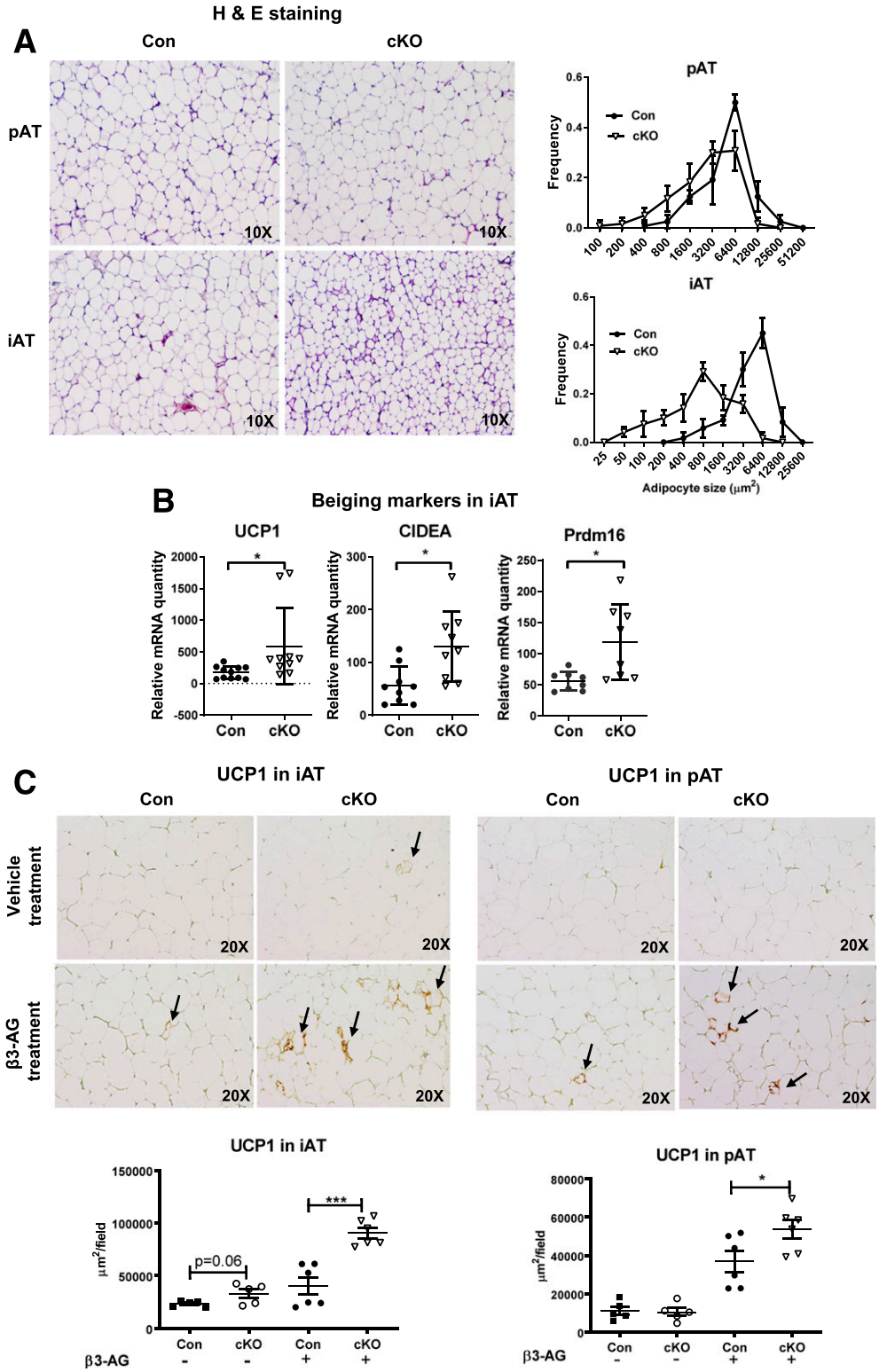

Figure 5—cKO mice fed HFD have enhanced AT browning and improved energy metabolism. Male cKO mice and littermate controls were fed HFD for 16 weeks. Representative hematoxylin and eosin (H & E) staining of pAT and iAT sections and quantitation of adipocyte size in pAT and iAT of cKO and control mice (*A*). mRNA levels of browning/beige adipogenesis markers examined by RT-qPCR in iAT of cKO and control mice (*B*). Representative immunohistochemistry staining and quantification of UCP1 expression in pAT and iAT of cKO and control mice treated with β3-agonist (β3-AG, CL316,243) or vehicle control (*C*). Comprehensive Lab Animal Monitoring System analysis of cKO mice and littermate controls showing VO_2 (*D*), respiratory exchange ratio (*E*), food intake (*F*), and activity (*G*). $n = 5$ mice/group. TG content quantified in the liver and skeletal muscle of cKO and control mice (*H*). $^*P < 0.05$, $^{***}P < 0.001$. Con, control.

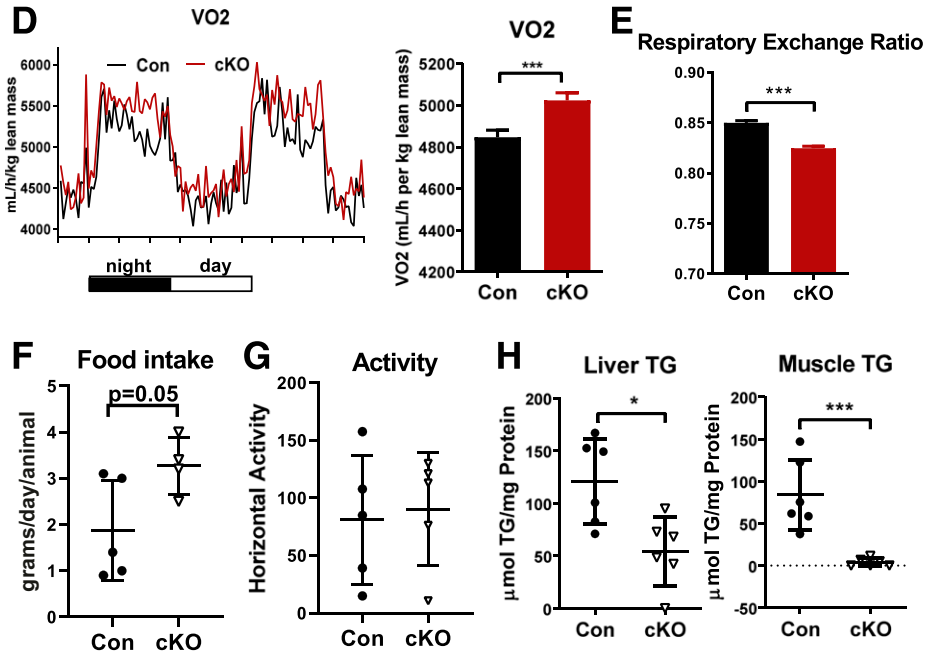

Figure 5—*Continued*.

time that Stat1 in MDCs plays a critical role in obesity-induced AT inflammation and insulin resistance. Consistently, short-term treatment with a Jak1/Jak2 inhibitor, which inhibits the Jak/Stat pathway, reduces inflammation and improves insulin resistance in mice with HFD-induced obesity (33) and lowers HbA_{1c} in humans with type 2 diabetes and diabetic kidney disease (34).

The dominant immune cell types of obese AT are macrophages and DCs (5–7,12,35,36) in which CD11c$^+$ MDCs, particularly CD11c$^+$ macrophages, are the predominant

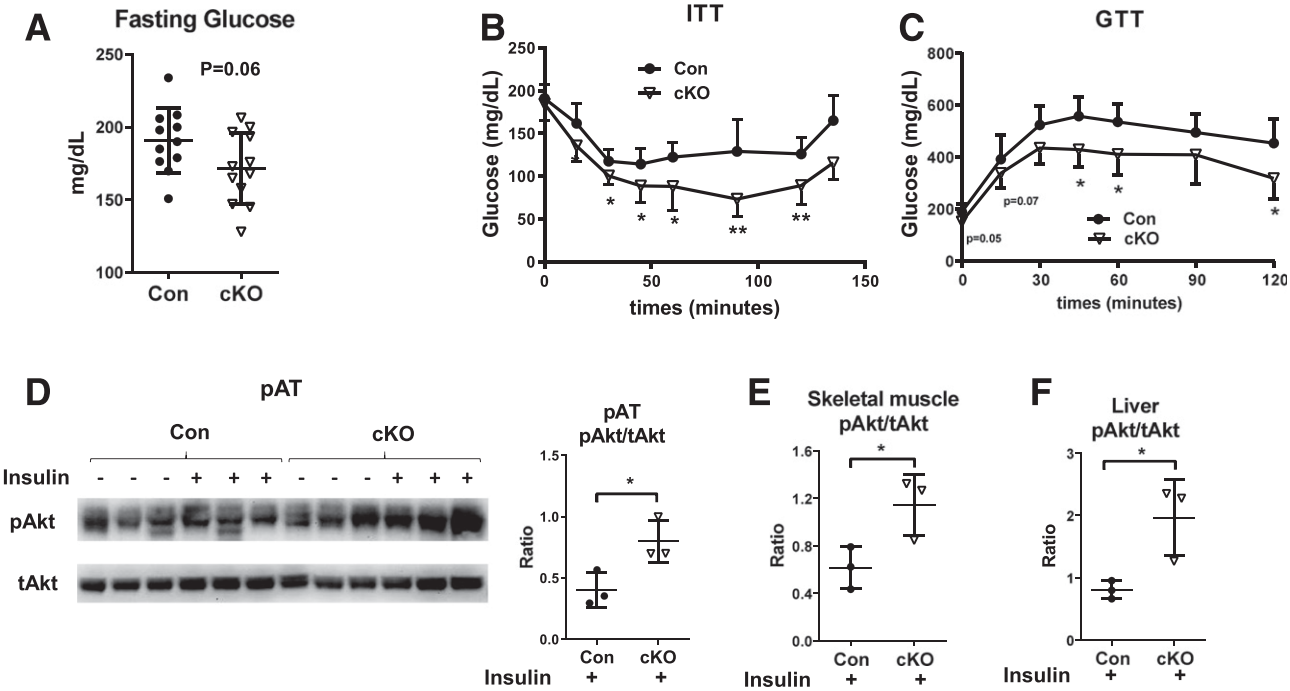

Figure 6—cKO mice on HFD have improved insulin resistance. Male cKO mice and littermate controls were fed HFD for 16 weeks. Blood glucose levels after fasting for 6 h (*A*). ITT (*B*). n = 6–8 mice/group. GTT (*C*). n = 5 mice/group. Insulin-induced Akt phosphorylation determined by Western immunoblot analysis in pAT (*D*), skeletal muscle (*E*), and liver (*F*). *$P < 0.05$, **$P < 0.01$. Con, control.

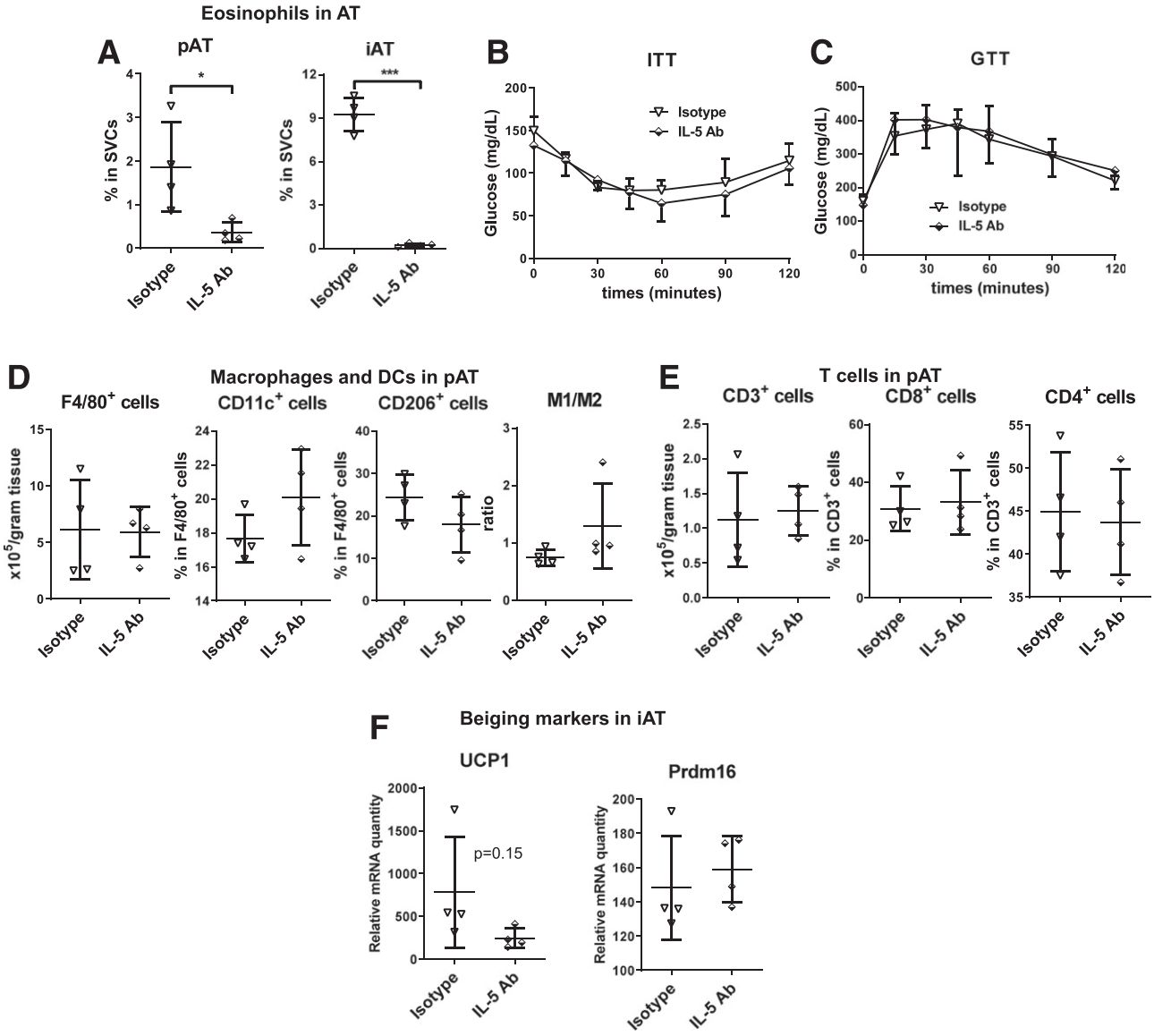

Figure 7—Reducing eosinophils does not affect insulin sensitivity in HFD-fed cKO mice. Male cKO mice that had been fed HFD for 12 weeks were injected intraperitoneally with 40 μg of anti-mouse IL-5 antibody (Ab) or isotype control once every 72 h for a total of 11 injections. Eosinophil content in pAT and iAT analyzed using flow cytometry at 2 days after the 11th injection (*A*). ITT performed at 2 days after the ninth injection (*B*). $n = 4$ mice/group. GTT performed at 2 days after the 10th injection (*C*). $n = 4$ mice/group. Macrophages and DCs (*D*) and T cells (*E*) analyzed using flow cytometry and mRNA levels of UCP1 and Prdm16 examined by RT-qPCR (*F*) in AT at 2 days after the 11th injection. $^{*}P < 0.05$, $^{***}P < 0.001$.

type and exhibit an M1-like phenotype (8–10,12–15, 35–38). Our study reveals a novel transcriptional mechanism for AT CD11c^{+} MDC, mainly CD11c^{+} macrophage, phenotypic change and its consequences on AT inflammation and metabolic functions in obesity.

HFD feeding in WT mice induced early and persistent increases of Stat1 expression and phosphorylation in AT and AT MDCs. Ablation of Stat1 in MDCs resulted in a reduction in MDC, particularly CD11c^{+} macrophage, M1-like polarization in pAT and iAT, supporting a critical role of Stat1 in obesity-induced AT MDC M1-like polarization and inflammation. On the basis of the crosstalk among various immune cell populations in obese AT, we attributed the changes in other immune cells, particularly T cells, to the phenotypic changes in MDCs in cKO mice. In particular, IL-12 is a major type 1 cytokine secreted by MDCs that augments T-cell activation and IFN-γ production (39). Therefore, the reduction in IL-12 expression by MDCs in AT of obese cKO mice may be the major reason for the decreases in IFN-γ–expressing T cells in AT of cKO mice. Moreover, IL-12 can inhibit Th2 responses (39). Therefore, the reduction in IL-12–expressing MDCs in AT of cKO mice may also explain the increase in Th2 cells. Hence, reduced IL-12 expression by MDCs, particularly CD11c^{+} macrophages, may underlie the decreased Th1 but augmented Th2 cells in AT of cKO mice on HFD. In

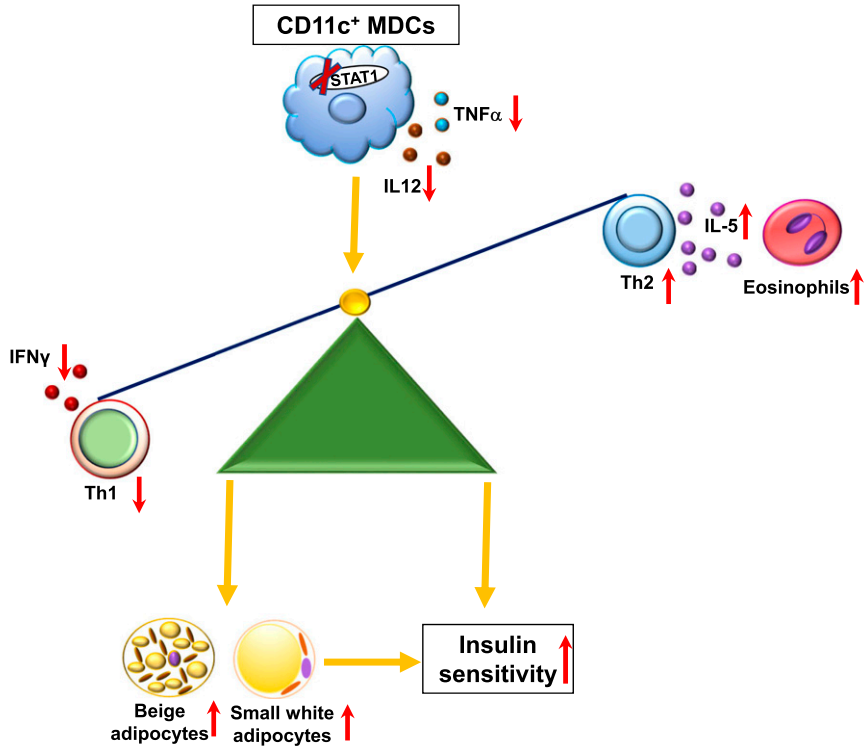

Figure 8—Potential mechanisms for alterations in AT inflammation and improvements in insulin sensitivity in mice with STAT1 ablation in MDCs.

addition, the increases in IL-5–expressing Th2 may explain the expansion of eosinophils in AT of cKO mice as supported by our observation that antibody neutralization of IL-5 dramatically reduced AT eosinophils in cKO mice on HFD. In contrast to the changes in AT, immune cells did not change significantly in the spleen of cKO mice. This may be because of differences in tissue environment, which play important roles in immune cell homeostasis. For example, obesity in WT mice enhances Th1 in pAT but not in spleen (20,33,40). Obesity reduces Tregs in pAT, but not in iAT and spleen (41). This may also explain the difference in some changes between pAT and iAT of cKO mice (Figs. 3 and 4).

Along with the above inflammatory changes in AT, obese cKO mice exhibited enhanced white AT browning and increased energy expenditure. Increased food intake may compensate to maintain the weight gain of cKO mice similar to control mice. Nevertheless, compared with controls, cKO mice had smaller adipocytes in both pAT and iAT, possibly representing a healthier phenotype of adipocytes. Furthermore, cKO mice had ameliorated ectopic lipid deposition in the liver and skeletal muscle evidenced by reduced TG content in these tissues, likely because of reduced lipid influx from "healthier" AT depots. Various immune cells may regulate AT browning in different ways. Although studies of the effects of M2 macrophages and eosinophils on promoting AT browning have generated inconsistent results (42–45), M1 macrophages and $CD8^+$ T cells have been implicated in repressing AT browning (46–48). Therefore, reduced type 1 inflammation, possibly in combination with increased type 2 inflammation, may underlie the enhanced AT browning in cKO mice.

The improvement of insulin resistance in cKO mice may stem from several mechanisms (Fig. 8). First, inflammatory molecules such as type 1 cytokines, including TNF-α and IFN-γ, which are mainly secreted by immune cells in AT (5,19,20,27), can directly impair insulin signaling, causing insulin resistance in a variety of cells/tissues such as adipocytes and skeletal muscle myocytes through paracrine and endocrine effects (49). Therefore, reductions in these inflammatory molecules may contribute to improved insulin resistance in cKO mice. In contrast, although eosinophils have been implicated in a protective role in obesity-linked insulin resistance (32), our data showing that reducing eosinophils did not alter insulin sensitivity in cKO mice do not support a major role of increased AT eosinophils in the improvement of insulin resistance in cKO mice. In support, a previous report showed that raising AT eosinophils in obese WT mice failed to rescue metabolic dysfunctions (45). In addition, ectopic lipid deposition, in the liver and skeletal muscle in particular, plays important roles in the development of tissue and systemic insulin resistance (49). Accordingly, reductions in lipid deposition in these tissues may also contribute to the improvement of insulin resistance in cKO mice. As supporting evidence, cKO mice compared with controls had improved insulin sensitivity not only in AT but also in skeletal muscle and liver. Furthermore, in cKO mice, the expansion of beige

adipocytes within white AT along with increased expression of UCP1 mediates nonshivering thermogenesis, which may further mitigate obesity-induced metabolic dysfunctions by increasing energy expenditure, substrate metabolism, and glucose homeostasis (50).

A limitation of the current study is that in cKO mice, STAT1 is deficient not only in AT $CD11c^+$ cells but also in $CD11c^+$ cells in other tissues. Although we observed changes in immune cells in AT, but not in spleens (macrophages and T cells) or bone marrow (eosinophils), of cKO mice, we cannot exclude potential changes in other tissues such as the liver, brain, and intestine, which may also affect systemic metabolism.

Taken together, our results demonstrate that Stat1 ablation in MDCs protects mice from obesity-induced AT MDC, particularly $CD11c^+$ macrophage, M1-like polarization and inflammation, leading to improvements in energy expenditure, insulin resistance, and metabolic functions. Therefore, our study supports a pivotal role of MDC Stat1 in obesity-linked inflammation and insulin resistance and indicates that targeting STAT1 could be a potential therapeutic strategy for obesity-induced metabolic dysfunctions.

Acknowledgments. The authors thank Kerrie Jara, Baylor College of Medicine, for editorial assistance.

Funding. This work was supported by National Institute of Diabetes and Digestive and Kidney Diseases grants R01-DK-114356 (to S.M.H.) and R01-DK-121348 (to H.W.); National Heart, Lung, and Blood Institute grant R01-HL-098839 (to H.W.); American Diabetes Association awards 1-18-IBS-105 (to S.M.H.) and 1-17-IBS-082 (to H.W.); and American Heart Association award 16GRNT30410012 (to H.W.).

Duality of Interest. No potential conflicts of interest relevant to this article were reported.

Author Contributions. A.A. performed the experiments, analyzed data, and wrote the manuscript. A.A. and H.W. designed the experiments. Z.L. performed the experiments, collected data, and edited the manuscript. X.D.P., J.P., H.L., A.R.C., and P.S. helped to perform the experiments and collect data. L.H. contributed to the experiments and edited the manuscript. S.M.H. and C.M.B. contributed to the experimental design and edited the manuscript. H.W. edited the manuscript. H.W. is the guarantor of this work and, as such, had full access to all the data in the study and takes responsibility for the integrity of the data and the accuracy of the data analysis.

Prior Presentation. Parts of the study were presented in abstract form at the 78th Scientific Sessions of the American Diabetes Association, Orlando, FL, 22–26 June 2018, and the 79th Scientific Sessions of the American Diabetes Association, San Francisco, CA, 7–11 June 2019.

References

1. Blüher M. Obesity: global epidemiology and pathogenesis. Nat Rev Endocrinol 2019;15:288–298
2. Hotamisligil GS. Inflammation, metaflammation and immunometabolic disorders. Nature 2017;542:177–185
3. Osborn O, Olefsky JM. The cellular and signaling networks linking the immune system and metabolism in disease. Nat Med 2012;18:363–374
4. Wu H, Ballantyne CM. Metabolic inflammation and insulin resistance in obesity. Circ Res 2020;126:1549–1564
5. Weisberg SP, McCann D, Desai M, Rosenbaum M, Leibel RL, Ferrante AW Jr. Obesity is associated with macrophage accumulation in adipose tissue. J Clin Invest 2003;112:1796–1808
6. Xu H, Barnes GT, Yang Q, et al. Chronic inflammation in fat plays a crucial role in the development of obesity-related insulin resistance. J Clin Invest 2003;112:1821–1830
7. Cancello R, Tordjman J, Poitou C, et al. Increased infiltration of macrophages in omental adipose tissue is associated with marked hepatic lesions in morbid human obesity. Diabetes 2006;55:1554–1561
8. Lumeng CN, Bodzin JL, Saltiel AR. Obesity induces a phenotypic switch in adipose tissue macrophage polarization. J Clin Invest 2007;117:175–184
9. Nguyen MT, Favelyukis S, Nguyen AK, et al. A subpopulation of macrophages infiltrates hypertrophic adipose tissue and is activated by free fatty acids via Toll-like receptors 2 and 4 and JNK-dependent pathways. J Biol Chem 2007;282:35279–35292
10. Wu H, Perrard XD, Wang Q, et al. CD11c expression in adipose tissue and blood and its role in diet-induced obesity. Arterioscler Thromb Vasc Biol 2010;30:186–192
11. Wu H, Gower RM, Wang H, et al. Functional role of CD11c+ monocytes in atherogenesis associated with hypercholesterolemia. Circulation 2009;119:2708–2717
12. Cho KW, Zamarron BF, Muir LA, et al. Adipose tissue dendritic cells are independent contributors to obesity-induced inflammation and insulin resistance. J Immunol 2016;197:3650–3661
13. Li P, Lu M, Nguyen MT, et al. Functional heterogeneity of CD11c-positive adipose tissue macrophages in diet-induced obese mice. J Biol Chem 2010;285:15333–15345
14. Prieur X, Mok CY, Velagapudi VR, et al. Differential lipid partitioning between adipocytes and tissue macrophages modulates macrophage lipotoxicity and M2/M1 polarization in obese mice. Diabetes 2011;60:797–809
15. Porsche CE, Delproposto JB, Patrick E, Zamarron BF, Lumeng CN. Adipose tissue dendritic cell signals are required to maintain T cell homeostasis and obesity-induced expansion. Mol Cell Endocrinol 2020;505:110740
16. Lawrence T, Natoli G. Transcriptional regulation of macrophage polarization: enabling diversity with identity. Nat Rev Immunol 2011;11:750–761
17. Murray PJ. The JAK-STAT signaling pathway: input and output integration. J Immunol 2007;178:2623–2629
18. Rhee SH, Jones BW, Toshchakov V, Vogel SN, Fenton MJ. Toll-like receptors 2 and 4 activate STAT1 serine phosphorylation by distinct mechanisms in macrophages. J Biol Chem 2003;278:22506–22512
19. Jiang E, Perrard XD, Yang D, et al. Essential role of CD11a in CD8+ T-cell accumulation and activation in adipose tissue. Arterioscler Thromb Vasc Biol 2014;34:34–43
20. Khan IM, Dai Perrard XY, Perrard JL, et al. Attenuated adipose tissue and skeletal muscle inflammation in obese mice with combined CD4+ and CD8+ T cell deficiency. Atherosclerosis 2014;233:419–428
21. Wu H, Ghosh S, Perrard XD, et al. T-cell accumulation and regulated on activation, normal T cell expressed and secreted upregulation in adipose tissue in obesity. Circulation 2007;115:1029–1038
22. Shi H, Kokoeva MV, Inouye K, Tzameli I, Yin H, Flier JS. TLR4 links innate immunity and fatty acid-induced insulin resistance. J Clin Invest 2006;116:3015–3025
23. Himes RW, Smith CW. Tlr2 is critical for diet-induced metabolic syndrome in a murine model. FASEB J 2010;24:731–739
24. Klover PJ, Muller WJ, Robinson GW, Pfeiffer RM, Yamaji D, Hennighausen L. Loss of STAT1 from mouse mammary epithelium results in an increased Neu-induced tumor burden. Neoplasia 2010;12:899–905
25. Wang J, Perrard XD, Perrard JL, et al. ApoE and the role of very low density lipoproteins in adipose tissue inflammation. Atherosclerosis 2012;223:342–349
26. Wu H, Rodgers JR, Perrard XY, et al. Deficiency of CD11b or CD11d results in reduced staphylococcal enterotoxin-induced T cell response and T cell phenotypic changes. J Immunol 2004;173:297–306
27. Nishimura S, Manabe I, Nagasaki M, et al. CD8+ effector T cells contribute to macrophage recruitment and adipose tissue inflammation in obesity. Nat Med 2009;15:914–920
28. Cho KW, Morris DL, DelProposto JL, et al. An MHC II-dependent activation loop between adipose tissue macrophages and CD4+ T cells controls obesity-induced inflammation. Cell Rep 2014;9:605–617
29. Morris DL, Cho KW, Delproposto JL, et al. Adipose tissue macrophages function as antigen-presenting cells and regulate adipose tissue CD4+ T cells in mice. Diabetes 2013;62:2762–2772

30. Morris DL, Oatmen KE, Mergian TA, et al. CD40 promotes MHC class II expression on adipose tissue macrophages and regulates adipose tissue CD4+ T cells with obesity. J Leukoc Biol 2016;99:1107–1119
31. Deng T, Lyon CJ, Minze LJ, et al. Class II major histocompatibility complex plays an essential role in obesity-induced adipose inflammation. Cell Metab 2013;17:411–422
32. Wu D, Molofsky AB, Liang HE, et al. Eosinophils sustain adipose alternatively activated macrophages associated with glucose homeostasis. Science 2011;332: 243–247
33. Khan IM, Perrard XY, Brunner G, et al. Intermuscular and perimuscular fat expansion in obesity correlates with skeletal muscle T cell and macrophage infiltration and insulin resistance. Int J Obes 2015;39:1607–1618
34. Tuttle KR, Brosius FC III, Adler SG, et al. JAK1/JAK2 inhibition by baricitinib in diabetic kidney disease: results from a phase 2 randomized controlled clinical trial. Nephrol Dial Transplant 2018;33:1950–1959
35. Lumeng CN, Saltiel AR. Inflammatory links between obesity and metabolic disease. J Clin Invest 2011;121:2111–2117
36. McNelis JC, Olefsky JM. Macrophages, immunity, and metabolic disease. Immunity 2014;41:36–48
37. Shaul ME, Bennett G, Strissel KJ, Greenberg AS, Obin MS. Dynamic, M2-like remodeling phenotypes of CD11c+ adipose tissue macrophages during high-fat diet–induced obesity in mice. Diabetes 2010;59:1171–1181
38. Wentworth JM, Naselli G, Brown WA, et al. Pro-inflammatory CD11c+CD206+ adipose tissue macrophages are associated with insulin resistance in human obesity. Diabetes 2010;59:1648–1656
39. O'Garra A, Murphy KM. From IL-10 to IL-12: how pathogens and their products stimulate APCs to induce T(H)1 development. Nat Immunol 2009;10:929–932
40. Winer S, Chan Y, Paltser G, et al. Normalization of obesity-associated insulin resistance through immunotherapy. Nat Med 2009;15:921–929
41. Feuerer M, Herrero L, Cipolletta D, et al. Lean, but not obese, fat is enriched for a unique population of regulatory T cells that affect metabolic parameters. Nat Med 2009;15:930–939
42. Qiu Y, Nguyen KD, Odegaard JI, et al. Eosinophils and type 2 cytokine signaling in macrophages orchestrate development of functional beige fat. Cell 2014;157:1292–1308
43. Nguyen KD, Qiu Y, Cui X, et al. Alternatively activated macrophages produce catecholamines to sustain adaptive thermogenesis. Nature 2011; 480:104–108
44. Fischer K, Ruiz HH, Jhun K, et al. Alternatively activated macrophages do not synthesize catecholamines or contribute to adipose tissue adaptive thermogenesis. Nat Med 2017;23:623–630
45. Bolus WR, Peterson KR, Hubler MJ, Kennedy AJ, Gruen ML, Hasty AH. Elevating adipose eosinophils in obese mice to physiologically normal levels does not rescue metabolic impairments. Mol Metab 2018;8:86–95
46. Sakamoto T, Nitta T, Maruno K, et al. Macrophage infiltration into obese adipose tissues suppresses the induction of UCP1 level in mice. Am J Physiol Endocrinol Metab 2016;310:E676–E687
47. Chung KJ, Chatzigeorgiou A, Economopoulou M, et al. A self-sustained loop of inflammation-driven inhibition of beige adipogenesis in obesity. Nat Immunol 2017;18:654–664
48. Moysidou M, Karaliota S, Kodela E, et al. CD8+ T cells in beige adipogenesis and energy homeostasis. JCI Insight 2018;3:e95456
49. Wu H, Ballantyne CM. Skeletal muscle inflammation and insulin resistance in obesity. J Clin Invest 2017;127:43–54
50. Sidossis L, Kajimura S. Brown and beige fat in humans: thermogenic adipocytes that control energy and glucose homeostasis. J Clin Invest 2015;125: 478–486